

# Molecular and clinical insights from studies of calcium-sensing receptor mutations

Gorvin, Caroline M

DOI:

[10.1530/JME-19-0104](https://doi.org/10.1530/JME-19-0104)

License:

None: All rights reserved

*Document Version*

Peer reviewed version

*Citation for published version (Harvard):*

Gorvin, CM 2019, 'Molecular and clinical insights from studies of calcium-sensing receptor mutations', *Journal of Molecular Endocrinology*, vol. 63, no. 2, pp. R1-R16. <https://doi.org/10.1530/JME-19-0104>

[Link to publication on Research at Birmingham portal](#)

## **Publisher Rights Statement:**

This manuscript has been accepted for publication in *Journal of Molecular Endocrinology*, but the version presented here has not yet been copy-edited, formatted or proofed. Consequently, Bioscientifica accepts no responsibility for any errors or omissions it may contain. The definitive version is now freely available at <https://doi.org/10.1530/JME-19-0104> 2019

## **General rights**

Unless a licence is specified above, all rights (including copyright and moral rights) in this document are retained by the authors and/or the copyright holders. The express permission of the copyright holder must be obtained for any use of this material other than for purposes permitted by law.

- Users may freely distribute the URL that is used to identify this publication.
- Users may download and/or print one copy of the publication from the University of Birmingham research portal for the purpose of private study or non-commercial research.
- User may use extracts from the document in line with the concept of 'fair dealing' under the Copyright, Designs and Patents Act 1988 (?)
- Users may not further distribute the material nor use it for the purposes of commercial gain.

Where a licence is displayed above, please note the terms and conditions of the licence govern your use of this document.

When citing, please reference the published version.

## **Take down policy**

While the University of Birmingham exercises care and attention in making items available there are rare occasions when an item has been uploaded in error or has been deemed to be commercially or otherwise sensitive.

If you believe that this is the case for this document, please contact [UBIRA@lists.bham.ac.uk](mailto:UBIRA@lists.bham.ac.uk) providing details and we will remove access to the work immediately and investigate.

1 **Molecular and clinical insights from studies of calcium-sensing receptor mutations**

2 Caroline M. Gorvin<sup>a,b,c</sup>

3

4 **Author affiliations**

5 <sup>a</sup>Institute of Metabolism and Systems Research (IMSR), University of Birmingham, Birmingham, B15  
6 2TT, UK

7 <sup>b</sup>Centre of Membrane Proteins and Receptors (COMPARE), University of Birmingham, Birmingham,  
8 B15 2TT, UK

9 <sup>c</sup>Centre for Endocrinology, Diabetes and Metabolism (CEDAM), Birmingham Health Partners,  
10 Birmingham, B15 2TH, UK

11 Email: [C.Gorvin@bham.ac.uk](mailto:C.Gorvin@bham.ac.uk)

12 Telephone: +44 (0)121 414 6857

13

14 **Short Title:** Mutation landscape of the CaSR

15

16

17

18

19 **ABSTRACT**

20 Twenty-five years have elapsed since the calcium-sensing receptor (CaSR) was first identified in bovine  
21 parathyroid and the receptor is now recognized as a fundamental contributor to extracellular  $\text{Ca}^{2+}$  ( $\text{Ca}^{2+}_e$ )  
22 homeostasis, regulating parathyroid hormone release and urinary calcium excretion. The CaSR is a class  
23 C G-protein-coupled receptor (GPCR) that is functionally active as a homodimer and couples to  
24 multiple G-protein subtypes to activate intracellular signalling pathways. The importance of the CaSR  
25 in the regulation of  $\text{Ca}^{2+}_e$  has been highlighted by the identification of >400 different germline loss- and  
26 gain-of-function CaSR mutations that give rise to disorders of  $\text{Ca}^{2+}_e$  homeostasis. CaSR inactivating  
27 mutations cause neonatal severe hyperparathyroidism, characterised by marked hypercalcaemia,  
28 skeletal demineralisation and failure to thrive in early infancy; and familial hypocalciuric  
29 hypercalcaemia, an often asymptomatic disorder associated with mild-moderately elevated serum  
30 calcium concentrations. Activating mutations are associated with autosomal dominant hypocalcaemia,  
31 which is occasionally associated with a Bartter's-like phenotype. Recent elucidation of the CaSR  
32 extracellular domain structure enabled the locations of CaSR mutations to be mapped and has revealed  
33 clustering in locations important for structural integrity, receptor dimerisation and ligand-binding.  
34 Moreover, the study of disease-causing mutations has demonstrated that CaSR signals in a biased  
35 manner and have revealed specific residues important for receptor activation. This review presents the  
36 current understanding of the genetic landscape of CaSR mutations by summarising findings from  
37 clinical and functional studies of disease-associated mutations. It concludes with reflections on how  
38 recently uncovered signaling pathways may expand understanding of calcium homeostasis disorders.

39

40

41

42

43

## 44 **Discovery of the calcium-sensing receptor**

45           The significance of the parathyroid in calcium homeostasis has been recognised for more than  
46 100 years. Early investigations demonstrated that removal of the parathyroid glands induces acute  
47 hypocalcaemia in humans and animals and that intravenous injection of parathyroid gland extract or  
48 parathyroid hormone (PTH) normalises serum calcium levels (Conigrave 2016). Several decades later,  
49 isolated dispersed human parathyroid cell cultures were used to show that exogenous treatment with  
50  $\text{Ca}^{2+}$  or  $\text{Mg}^{2+}$  robustly reduced PTH secretion, leading to the proposal that parathyroid cells harbour a  
51  $\text{Ca}^{2+}$  sensor (Conigrave 2016). The molecular details of this calcium-sensing mechanism began to be  
52 uncovered in the late 1980s with the demonstration that divalent cations could induce inositol  
53 trisphosphate ( $\text{IP}_3$ ) **generation** and transient increases in intracellular calcium ( $\text{Ca}^{2+}_i$ ) in parathyroid  
54 cells, likely by a cell surface receptor (Nemeth and Scarpa 1987; Shoback, et al. 1988). Finally, in 1993,  
55 a 5.3kb clone, predicted to encode a protein of the G-protein-coupled receptor (GPCR) superfamily,  
56 was isolated from bovine parathyroid that when expressed in *Xenopus* oocytes had pharmacological  
57 properties similar to those of the calcium-sensing protein previously described in parathyroid cells  
58 (Brown, et al. 1993). Subsequently, orthologs of the protein, now known as the calcium-sensing  
59 receptor (CaSR), were cloned from several mammalian species, including humans, and from a variety  
60 of tissues (Conigrave 2016).

61

## 62 **Structure and activation of CaSR**

63           We now understand the CaSR to be a class C GPCR, comprising 1078 amino acids, that  
64 primarily exists at cell surfaces as a disulphide-linked homodimer. Two crystal structures of the CaSR  
65 extracellular domain (ECD) were published in 2016 and uncovered details of the receptor activation  
66 mechanism, which shares similarities with the related metabotropic glutamate receptors (mGluRs) and  
67  $\text{GABA}_B\text{R}$  (Geng, et al. 2016). The ECD (amino acids 1-610) comprises a bi-lobed venus fly-trap  
68 domain (VFTD) and a cysteine-rich domain (CRD) (Geng et al. 2016; Zhang, et al. 2016) (Figure 1).  
69 In the inactive state, the two CaSR protomers interact primarily at the lobe 1-lobe 1 interface. On

70 activation, each protomer undergoes a 29° rotation, bringing the Lobe 2-Lobe 2 and CRD-CRD domains  
71 into closer proximity, and expands the homodimer interface (Geng et al. 2016) (Figure 1). Interactions  
72 across the homodimer occur at several sites and play a critical role in structural integrity and receptor  
73 activation. In the inactive state, these include two loops that are unique to CaSR (Figure 1). Loop 1  
74 stretches across the dimer interface from lobe 1 of one protomer to interact with a hydrophobic surface  
75 on the other protomer (Geng et al. 2016; Zhang et al. 2016). In loop 2, two  $\alpha$ -helices at the top of lobe  
76 1 reach across the interprotomer region to stabilise dimerization. This loop involves intermolecular  
77 disulfide bonds between two highly conserved cysteine residues (Cys129 and Cys131), and a  
78 surrounding hydrophobic region (Geng et al. 2016; Zhang et al. 2016).

79 The CaSR transmembrane domain (TMD, amino acids 611-863) comprises seven  
80 transmembrane helices, three extracellular loops (ECL1-3) and three intracellular loops (ICL1-3), and  
81 mediates G-protein activation; while amino acids 864-1078 form the intracellular domain (ICD), which  
82 can interact with several proteins that modulate CaSR signalling and cell surface expression (Bai, et al.  
83 1998; McCullough, et al. 2004; Zhang and Breitwieser 2005). Upon ligand binding CaSR activates  
84 multiple signalling pathways by coupling to several G-protein subtypes, but predominantly utilises: the  
85  $G_{i/o}$  pathway to suppress cAMP and activate mitogen-activated protein kinase (MAPK) cascades; and  
86 the  $G_{q/11}$  pathway, that activates  $Ca^{2+}_i$  mobilisations and MAPK signalling (Conigrave 2016).

87

88

### 89 **Mutations in the CaSR causes disorders of calcium homeostasis**

90 Following its molecular cloning, the importance of CaSR in regulating  $Ca^{2+}_e$  homeostasis was  
91 confirmed by the discovery that germline inactivating mutations in the receptor cause two  
92 hypercalcaemic disorders, neonatal severe hyperparathyroidism (NSHPT) and the milder familial  
93 hypocalciuric hypercalcaemia type-1 (FHH1) (Pollak, et al. 1993; Pollak, et al. 1994); while activating  
94 mutations cause autosomal dominant hypocalcaemia type-1 (ADH1). In the 25 years that have elapsed  
95 since CaSR was cloned, more than 400 different human mutations have been described, and studies of  
96 these mutant proteins has provided important molecular insights into how the receptor is activated and  
97 mediates signalling. Within this review I will discuss some lessons we have learnt by studying these

98 mutations, from clinical presentation to molecular mechanisms of receptor activation. Inclusion of all  
99 reported CaSR mutations within this review would be impossible, and therefore they are listed in  
100 Supplementary Table 1.

101

## 102 **Neonatal severe hyperparathyroidism (NSHPT)**

103 NSHPT (OMIM:239200) is a rare disorder in which affected infants present with marked  
104 hypercalcaemia, skeletal demineralisation and failure to thrive, and can be fatal if left untreated (Pollak  
105 et al. 1993). Observations of the coincidence of NSHPT and FHH1 in families, and parental  
106 consanguinity in many NSHPT kindreds, led investigators to suspect NSPHT was caused by  
107 homozygous mutations, while the milder FHH1 arose from heterozygous mutations of the same gene.  
108 Initial genetic investigations were consistent with this hypothesis and studies of a CaSR knockout  
109 mouse model, in which homozygous mice have markedly elevated serum calcium and PTH, parathyroid  
110 hyperplasia, retarded growth and premature death, while heterozygous mice have mild hypercalcaemia  
111 (Ho, et al. 1995), consistent with NSHPT and FHH, respectively, seemingly provided further evidence  
112 of this genetic dosage effect. However, while most of the ~45 described cases of NSHPT are due to  
113 homozygous (~75%) or compound heterozygous mutations (~10%), several cases of NSHPT have been  
114 described in patients with heterozygous mutations of CaSR (Supplementary Table 1). The six mutations  
115 reported in these patients (Arg185Gln, Arg227Leu, Arg551Lys, Ile555Thr, Cys582Tyr and Ser591Cys)  
116 occur in the ECD of the CaSR, and are located in regions that are critical for receptor activation (Geng  
117 et al. 2016; Zhang et al. 2016) (Figure 2A). These include the hinge region between lobes 1 and 2  
118 (Arg185), the lobe 2 homodimer interface (Arg227), and the CRD homodimer interface (Ile555 and  
119 Arg551), while the Cys582 and Ser591 residues are also located within the CRD (Geng et al. 2016;  
120 Zhang et al. 2016) (Figure 2A). These three regions undergo the largest conformational changes during  
121 transition from the inactive to the active state, and several of these residues form critical agonist-induced  
122 homodimer contacts upon receptor activation (Geng et al. 2016; Zhang et al. 2016). The heterozygous  
123 NSHPT mutant residues are predicted to disrupt these contacts, and have been shown *in vitro* to severely

124 impair receptor responses, despite normal cell surface expression (Bai, et al. 1996; Toke, et al. 2007;  
125 Wystrychowski, et al. 2005).

126           However, these are not the only mutations to occur in these critical regions. Indeed, FHH1  
127 mutations have been reported in several of these residues and it is therefore unlikely that the location of  
128 the residue per se determines whether a patient presents with NSHPT or FHH1. How mutations in a  
129 single residue cause the two different disorders has been examined for the Arg227 residue,  
130 demonstrating that the Arg227Leu mutation, which causes NSHPT, has a more severe impairment in  
131 receptor signalling compared to a mutation in the same residue, Arg227Gln, which causes FHH1  
132 (Wystrychowski et al. 2005). Therefore, for this residue at least, there appears to be a genotype-  
133 phenotype correlation to explain the differences in clinical presentation. Yet this is not consistent for  
134 all NSHPT heterozygous mutant residues as some mutations have been shown to cause NSHPT in one  
135 patient, while other patients have presented with FHH1 (Supplementary Table 1) (Nyweide, et al. 2006;  
136 Reh, et al. 2011; Taki, et al. 2015). Intrauterine exposure to maternal calcium and vitamin D, and the  
137 presence of other CaSR polymorphisms that could act as genetic modifiers to influence receptor  
138 activity, could explain the discrepancies of clinical presentation in some heterozygous patients (Reh et  
139 al. 2011; Taki et al. 2015; Toke et al. 2007).

140

#### 141 **Types of mutation and functional effect of NSHPT mutations**

142           Twenty-nine different homozygous mutations have been described in association with NSHPT,  
143 with almost half due to missense mutations (Supplementary Table 1). These missense mutations occur  
144 predominantly in the ECD (~84%), demonstrating the importance of this domain in receptor activation  
145 and maintaining structural integrity. Additionally, one homozygous NSHPT mutation (Gly768Val)  
146 occurs in ECL2 and this mutation is predicted to disrupt the tightly packed region between the CRD,  
147 ECL2 and TMD; while the only missense ICD mutation described to cause NSHPT, Arg886Trp, has  
148 an unknown effect on CaSR. The other 17 NSHPT mutations include 7 nonsense mutations, 5  
149 frameshifts resulting in a premature stop codon, 1 deletion, 1 insertion-deletion, 2 intronic variants  
150 resulting in changes in splice sites, and one insertion of an Alu repeat has also been reported in three

151 families (Figure 2B, Supplementary Table 1). All the nonsense mutations affect residues within the  
152 ECD, resulting in loss of the whole TMD and ICD, and subsequently complete loss of CaSR signalling.  
153 Similarly, many of the frameshift mutations and large deletions result in complete or partial loss of the  
154 TMD and total deletion of the ICD.

155 Fifteen of the NSHPT mutations have been characterised *in vitro*, including three of the  
156 heterozygous mutations (Supplementary Table 1). All mutations impair or abolish CaSR signalling (as  
157 measured by  $Ca^{2+}_i$ , MAPK and/or  $IP_3$  assays (measuring the  $IP_3$  breakdown product  $IP_1$ )). The majority  
158 of the homozygous mutations (6 of 7 tested) reduced cell surface expression, which may be due to  
159 failure of some CaSR mutants to complete quality control checks at the ER and Golgi (Huang and  
160 Breitwieser 2007), while none of the heterozygous mutations tested affect cell surface expression,  
161 indicating these mutations may impair receptor activation rather than protein expression.

162

### 163 **Clinical details and treatment of NSHPT**

164 Clinical biochemistry from 41 patients with NSHPT demonstrates a mean serum calcium of  
165  $4.80 \pm 1.79$  mmol/L (range of 2.8-9.2 mmol/L, normal range 2.2-2.6 mmol/L). Those individuals with  
166 homozygous mutations or compound heterozygous mutations have higher serum calcium values (mean,  
167  $5.68 \pm 1.81$  mmol/L and  $4.75 \pm 1.27$  mmol/L, respectively) than those with heterozygous mutations  
168 (mean,  $3.24 \pm 0.23$  mmol/L), demonstrating a mutation dosage effect, although a wide range of serum  
169 calcium values are observed in homozygous individuals (Figure 2C). Similarly, nonsense mutations and  
170 truncation mutations, which are likely to have a more devastating effect on receptor structure and  
171 consequently CaSR activity cause a more severe increase in serum calcium than missense mutations  
172 (Figure 2D). PTH values were higher than the normal range in 83% of NSHPT patients.

173 The median age of diagnosis of NSHPT is 14 days, with a large age range between 2 days and  
174 up to several months of age. Despite this range, there was no difference in the calcium values of patients  
175 presenting early (<2 weeks post-partum) and those presenting later (>2 weeks after birth) (mean,  
176  $4.80 \pm 1.95$  vs.  $4.74 \pm 1.72$  mmol/L, respectively), nor was there a difference in the type of symptoms with  
177 which these individuals presented. The most commonly reported symptoms were skeletal

178 undermineralisation and/or osteopenia (69.5%), failure to thrive (47.2%) and hypotonia (47.2%) (Figure  
179 2E). Respiratory distress and lethargy are also commonly observed (both 33.3%), while dehydration,  
180 constipation and nausea/ vomiting are observed in <20% in NSHPT patients (Figure 2E).  
181 Parathyroidectomy is often the preferred treatment option in NSHPT, with bisphosphonates used to  
182 reduce hypercalcaemia prior to surgery (Mayr, et al. 2016). Use of the CaSR positive allosteric  
183 modulator, cinacalcet, which enhances the sensitivity of the receptor to  $Ca^{2+}_e$ , have also been successful  
184 in lowering PTH and decreasing serum calcium in some NSHPT patients (Mayr et al. 2016; Sun, et al.  
185 2018) (Supplementary Table 1). Cinacalcet has proven effective in patients with the Arg185Gln  
186 heterozygous mutation, and some homozygous patients (e.g. Arg69His); however, other patients are  
187 unresponsive (e.g. Arg680His), indicating its efficacy is genotype-dependent (Mayr et al. 2016; Sun et  
188 al. 2018). Despite this caveat, cinacalcet is likely to be increasingly utilised as an initial treatment in  
189 NSHPT patients, due to its rapid effect on PTH levels and serum calcium.

190

#### 191 **Key messages for NSHPT**

- 192 • The majority of NSHPT mutations are homozygous, although heterozygous cases have been  
193 described.
- 194 • Heterozygous NSHPT mutations are located in regions that are critical for receptor activation  
195 and are associated with reduced serum calcium values compared to homozygous or compound  
196 heterozygous mutations.
- 197 • Cinacalcet is an effective treatment in some patients, although parathyroidectomy is routinely  
198 performed too.

199

#### 200 **Familial hypocalciuric hypercalcaemia type-1 (FHH1)**

201 Inactivating mutations in the CaSR also cause FHH1 (OMIM:145980), an autosomal dominant  
202 condition characterised by lifelong elevated serum calcium values, high or normal PTH concentrations  
203 and a low renal calcium excretion (Christensen, et al. 2008; Eastell, et al. 2014). FHH1 is usually benign

204 and does not require treatment, however, its biochemical features have considerable overlap with typical  
205 primary hyperparathyroidism (PHPT), and often FHH is classified as a form of atypical PHPT (Marx  
206 2018). However, unlike in typical PHPT, hypercalcaemia in FHH patients remains persistent following  
207 parathyroidectomy, and therefore it is important to distinguish between typical PHPT, and atypical  
208 forms (i.e. FHH) to avoid unnecessary surgery (Christensen et al. 2008; Eastell et al. 2014).  
209 Measurement of the urinary calcium/creatinine clearance ratio (UCCR) has been suggested as a simple  
210 biochemical diagnostic test to differentiate the two conditions with a cut-off of <0.02 for FHH1  
211 (Christensen et al. 2008). However, low UCCRs (between 0.01-0.02) are observed in some typical  
212 PHPT patients, especially those with vitamin D deficiency or renal insufficiency, therefore genetic  
213 analysis is still the gold-standard in differentiating between FHH1 and typical PHPT (Christensen et al.  
214 2008; Eastell et al. 2014). Despite this, a failure to identify a mutation in CaSR or other FHH-related  
215 genes may not indicate the patient has typical PHPT, as some FHH patients have no mutations in the  
216 currently known causative genes. Therefore, a combined approach with consideration of genetic  
217 analysis, UCCR and other symptoms may be best practice in ascertaining a correct diagnosis between  
218 FHH and typical PHPT patients.

219 Patients with FHH1 usually have mild hypercalcaemia; the mean serum calcium value of all  
220 FHH1 patients reported in >200 cases is  $2.85 \pm 0.28$  mmol/L, 31% of whom have a high serum PTH  
221 level. However, there is a wide range of serum calcium values from 2.43-4.48 mmol/L, with 177 patients  
222 with mild hypercalcaemia, 29 patients with moderate hypercalcaemia (3.1-3.5 mmol/L), and 6 patients  
223 with severe hypercalcaemia (>3.5 mmol/L). Indeed, it is becoming increasingly recognised that CaSR  
224 loss-of-function mutations are responsible for a spectrum of hypercalcaemic disorders, from serum  
225 calcium values slightly above the normal range to severe symptomatic hypercalcaemia similar to typical  
226 PHPT (Hannan and Thakker 2013). The majority of patients with FHH1 are asymptomatic (~71%).  
227 However some individuals have typical symptoms of hypercalcaemia including headaches, fatigue,  
228 muscle cramps, constipation, nausea and vomiting (9%), while other patients present with associated  
229 features including nephrocalcinosis/nephrolithiasis (~7%), osteoporosis and/or fractures (9%) and  
230 pancreatitis (3.5%). It is also possible that some of these associated symptoms are incidental and not  
231 caused by the CaSR mutation. Those individuals with symptomatic hypercalcaemia have higher serum

232 calcium values than those that are asymptomatic ( $2.97\pm 0.38$  vs.  $2.79\pm 0.17$  mmol/L, Figure 3A), and it  
233 is likely this hypercalcaemic spectrum will become even more apparent as more population level genetic  
234 data becomes available and the relationship between serum calcium concentration and CaSR variant  
235 status can be assessed in more detail. Treatment is not required in most cases of FHH, although  
236 cinacalcet has been shown to be efficacious in some individuals with symptomatic hypercalcaemia  
237 (Supplementary Table 1).

238

### 239 Genetic landscape of FHH1 mutations

240 Almost 300 mutations have been reported in association with FHH1. Of these ~81% are  
241 missense mutations, 6.5% are nonsense mutations, 8% are deletion mutations, while 7 intron mutations  
242 that cause splice-site changes and 7 insertion mutations have also been described (Figure 3B,  
243 Supplementary Table 1). The majority of these FHH1 mutations are heterozygous; however, there are  
244 a small number of cases in which homozygous mutations have been detected (Supplementary Table 1).  
245 These individuals present at an earlier age than other FHH1 patients and are born to consanguineous  
246 parents (Hannan, et al. 2010). The serum calcium values for homozygous FHH1 patients are  
247 significantly greater than those in heterozygous patients (Figure 3C). Functional analyses of  $Ca^{2+}_i$  show  
248 homozygous FHH1 mutants have a milder loss-of-function than those identified in the heterozygous  
249 state, and it is possible these mutations have a less severe effect on receptor function and consequently  
250 mutations on both alleles are necessary for an *in vivo* effect to become apparent (Chikatsu, et al. 1999;  
251 Hannan et al. 2010). Consistent with this, the heterozygous parents of individuals with homozygous  
252 FHH1 mutations are often normocalcaemic, and the mutations are not predicted to affect structural  
253 integrity or receptor activation (Hannan et al. 2010).

254

### 255 FHH1 ECD mutations

256 Of the 234 missense mutants, 155 are located in the ECD, 66 in the TMD and 13 in the ICD  
257 (Figure 3D). Missense mutations in the CaSR ECD cluster in three locations: loop 1, dimer interfaces  
258 and ligand-binding sites (Figure 4). Nine FHH1 mutations have been identified within loop 1 which

259 extends from Ile40 to Tyr63 and stretches across the homodimer interface to interact with a hydrophobic  
260 surface on the other protomer (Geng et al. 2016; Zhang et al. 2016) (Figure 1, Supplementary Table 1).  
261 Of note Pro55, which is mutated to Leu55 in FHH1, forms an interaction with residues on lobe 1 of the  
262 opposite protomer and is thought to contribute to dimerization (Zhang et al. 2016). *In vitro* studies have  
263 shown the Leu55 mutant reduces cell surface expression of the Pro55Leu mutant protein and impairs  
264 signalling (Chikatsu et al. 1999; White, et al. 2009).

265 Almost 70 FHH1 mutations are located at critical domain interfaces including 28 at the  
266 homodimer interface, 24 at the hinge region between lobe 1 and lobe 2, 8 at the interface between lobe  
267 2 and the CRD, and 11 at the CRD-CRD homodimer interface (Figure 4A, Supplementary Table 1).  
268 The dimer interface has two critical functions: structural integrity of the receptor and expansion of  
269 receptor contacts following agonist-induced conformational changes, which leads to activation of the  
270 receptor (Geng et al. 2016; White et al. 2009; Zhang et al. 2016). Consistent with these functions, 31%  
271 of FHH1 dimer interface mutations disrupt cell surface expression and all mutations tested disrupt both  
272  $Ca^{2+}_i$  and MAPK activity.

273 The final location at which FHH1 missense mutations cluster is the ligand-binding sites (Figure  
274 4A-E). Four distinct  $Ca^{2+}$ -binding sites have been identified in CaSR-ECD crystal structures: site 1  
275 located at the top of lobe 1; site 2 in lobe 1 above the interdomain crevice; site 3 in the cleft between  
276 lobe 1 and lobe 2; and site 4 within the lobe 2-CRD interface (Figure 4A) (Geng et al. 2016; Zhang et  
277 al. 2016). In addition, tryptophan can bind at an orthosteric site within the interdomain interface in the  
278 active state and acts as a co-agonist to facilitate ECD closure to potentiate CaSR function (Geng et al.  
279 2016; Zhang et al. 2016). Forty-six FHH1 missense mutations map within  $10\text{\AA}$  of a  $Ca^{2+}$  or L-Trp  
280 binding site, and could potentially affect ligand binding (Figure 4B-E). Several residues have been  
281 shown to directly coordinate  $Ca^{2+}$ -binding including: Ile81 in site 1 (mutated to Thr81 and Met81 in  
282 FHH1); Thr100 and Thr145 in site 2 (both mutated to isoleucines in FHH1); Arg66 and Ser302 in site  
283 3 (mutated to His66, Cys66 and Phe302 in FHH1); and Glu231 and Gly557 in site 4 (mutated to Lys231  
284 and Glu557 in FHH1) (Figure 4B-E, Supplementary Table 1). All these mutations have been shown to  
285 impair receptor signalling *in vitro* (Geng et al. 2016; Zhang et al. 2016). Furthermore, several residues  
286 including Thr145, Tyr218, Ser296, Glu297 and Ala298, which are the site of seven FHH1 mutations,

287 are involved in L-Trp binding, and these mutations similarly impair receptor activation (Geng et al.  
288 2016).

289

### 290 **FHH1 mutations in the TMD**

291 Sixty-six FHH1 mutations are located in the TMD (Supplementary Table 1). Using the crystal  
292 structure of the related class C GPCR, mGluR5 (Dore, et al. 2014), it is possible to build a homology  
293 model of the CaSR-TMD and discern the likely locations of the FHH1 mutations within the TMD  
294 (Figure 5). Previous studies of loss-of-function mutations in other GPCRs has shown a clustering at the  
295 TM1-TM2-TM7 interface, and at the TM3-TM6 interface (Stoy and Gurevich 2015). CaSR inactivating  
296 mutations identified in FHH1 similarly cluster in the TM1-TM2-TM7 interface (16 FHH1 mutations,  
297 Figure 5A). There is no clustering at the TM3-TM6 interface, although there are two independent groups  
298 of mutations surrounding TM3 (27 mutations) and TM6 (20 mutations) (Figure 5B-C). Within other  
299 class C GPCRs, TM3 and TM6 undergo large ligand-induced conformational changes, which is  
300 necessary for receptor activation and G-protein coupling, and FHH1 mutations may impair these  
301 structural changes, consequently impairing receptor signalling (Binet, et al. 2007; Leach, et al. 2012;  
302 Xue, et al. 2015).

303

### 304 **Key messages for FHH**

- 305 • Usually associated with mild hypercalcaemia, but is increasingly becoming recognised that  
306 loss-of-function CaSR mutations are responsible for a spectrum of hypercalcaemic disorders
- 307 • Majority of patients are asymptomatic, and those patients that have hypercalcaemic symptoms  
308 have higher serum calcium values
- 309 • More than 300 mutations have been described to cause FHH, the majority of which are missense
- 310 • ECD mutations cluster in three locations: loop 1, dimer interfaces and ligand-binding sites
- 311 • TMD mutations cluster in the TM1-TM2-TM7 interface or surrounding TM3 and TM6

312

### 313 **CaSR gain-of-function mutations cause ADH1**

314 ADH1 (OMIM:601198), caused by gain-of function mutations in CaSR, is characterised by  
315 mild to moderate hypocalcaemia associated with inappropriately low or normal serum PTH values  
316 (Hannan and Thakker 2013; Roszko, et al. 2016). In the population of ADH1 patients described to date  
317 (~100 patients, Supplementary Table 1), the mean serum calcium value is  $1.68 \pm 0.31$  mmol/L with a  
318 range of 0.79-2.3 mmol/L. In these patients serum PTH concentrations are inappropriately low in 76%  
319 of patients and normal in 24% of patients. Other biochemical features of ADH1 include  
320 hyperphosphatemia, hypomagnesemia and hypercalciuria (Hannan and Thakker 2013; Roszko et al.  
321 2016). Most ADH1 patients have a urinary calcium to creatinine ratio within or above the reference  
322 range and relative hypercalciuria arises as the low levels of PTH fail to induce calcium reabsorption  
323 from the primary filtrate at the kidney (Roszko et al. 2016). Patients with ADH1 need to be distinguished  
324 from individuals with other forms of hypoparathyroidism as treatment with vitamin D or its metabolites  
325 to correct hypocalcaemia may exacerbate hypercalciuria and nephrocalcinosis in ADH1 patients  
326 (Hannan and Thakker 2013; Roszko et al. 2016). In asymptomatic individuals treatment is therefore  
327 avoided. In those patients with symptomatic hypocalcaemia alternative treatments include thiazide  
328 diuretics, which lower urinary calcium, or recombinant human PTH (Hannan and Thakker 2013;  
329 Roszko et al. 2016). Future treatments of symptomatic ADH1 are likely to include negative allosteric  
330 modulators of the CaSR (calcilytics), which have been demonstrated to normalise calcium responses *in*  
331 *vitro*, and to increase serum PTH and calcium, while reducing urinary calcium excretion in mouse  
332 models of ADH1 (Dong, et al. 2015).

333 ADH1 is asymptomatic in 28% of patients. Most symptoms observed in ADH1 patients are due  
334 to neuromuscular irritability caused by hypocalcaemia and include carpopedal spasms, tetany,  
335 paraesthesia and seizures (Raue, et al. 2011). Seizures have been described in 39% of ADH1 patients  
336 with other hypocalcaemic features reported in 41%. Additionally, some patients present with associated  
337 features including basal ganglia calcifications (32%) and nephrocalcinosis (36%). The severity of  
338 hypocalcaemia correlates with the observance of symptomatic ADH1 with such individuals presenting

339 with a significantly lower serum calcium concentration than those without symptoms ( $1.65\pm 0.33$   
340 mmol/L vs.  $1.82\pm 0.23$  mmol/L, Figure 6A).

341

## 342 Genetic landscape of ADH1

343 Accurate diagnosis of ADH1 requires CaSR mutational analysis. To date, 100 different  
344 mutations have been described that are associated with ADH1 (Supplementary Table 1). The majority  
345 of cases (96%) are caused by heterozygous missense mutations (Figure 6B, Supplementary Table 1).  
346 However, one nonsense mutation (Gln934Stop) and four deletions (Ser895fsX939, del:Ser895-  
347 Val1075, Ser901fsX977 and Leu968fsX977) that occur in the ICD have also been described in ADH1.  
348 These four mutations result in loss of >100 amino acids within the C-terminus, indicating that this  
349 region of the CaSR is critical for receptor desensitisation or degradation. Indeed, two ubiquitin ligases,  
350 AMSH and dorfins, which reduce CaSR expression by increasing receptor degradation, have been  
351 demonstrated to bind to this region of the C-terminus (Huang, et al. 2006; McCullough et al. 2004), and  
352 the ADH1 deletion mutants may increase CaSR signalling by reducing receptor degradation. Consistent  
353 with this idea, *in vitro* studies demonstrated that cells expressing the Ser895fsX939 and Ser901-  
354 904fsX977 mutants exhibited elevated levels of CaSR protein and increased  $Ca^{2+}_i$  and MAPK signalling  
355 when compared to cells expressing wild-type CaSR (Lienhardt, et al. 2000; Maruca, et al. 2017;  
356 Obermannova, et al. 2016). This occurs despite loss of the region identified to bind filamin-A, an actin  
357 cytoskeletal protein that enhances CaSR-mediated activation of MAPK pathways (Zhang and  
358 Breitwieser 2005). Therefore, many questions remain to be answered regarding how truncation of the  
359 CaSR C-terminal tail by ADH1 mutations promotes receptor signalling.

360 The 95 ADH1 missense mutations are predominantly located in the ECD (52 mutations) and  
361 TMD (41 mutations), with only two mutations identified in the C-terminal region (Figure 6C). There is  
362 no correlation between serum calcium values of individuals with mutations in the ECD, TMD or C-  
363 terminus, although the range of calcium values is wider for patients with ECD mutations ( $0.79\text{--}2.2$   
364 mmol/L compared to  $1.18\text{--}2.02$  mmol/L for C-terminus mutations) (Figure 6D). The two C-terminal  
365 missense mutations affect residues that are critical for facilitating  $Ca^{2+}_i$  responses (Bai et al. 1998;

366 Huang, et al. 2010; Lazarus, et al. 2011). The first mutation Val883Met, disrupts a region that is known  
367 to interact with calmodulin and dorfin (Huang et al. 2010), while the second mutation, Thr888Met,  
368 disrupts a protein kinase C phosphorylation site that negatively regulates CaSR coupling to Ca<sup>2+</sup><sub>i</sub>; stores  
369 (Bai et al. 1998). Mutation of this residue impairs receptor phosphorylation, and increases CaSR-  
370 mediated Ca<sup>2+</sup><sub>i</sub> and pERK signalling (Bai et al. 1998; Lazarus et al. 2011).

371         The ECD missense mutations are clustered in three key sites: loop 2; the hinge region between  
372 lobes 1 and 2; and the homodimer interface, demonstrating the importance of these residues in CaSR  
373 receptor activation and signalling (Figure 6E, Supplementary Table 1). Loop 2 stretches across the  
374 interprotomer region at each lobe 1 and stabilises dimerization (Geng et al. 2016; Zhang et al. 2016).  
375 Twenty-four ADH1 mutations have been reported within this region, and many of these residues are  
376 mutation hotspots, with some residues mutated multiple times in different patients (Supplementary  
377 Table 1). Two residues in particular, Cys129 and Cys131, are each mutated to four different amino  
378 acids, and *in vitro* studies have revealed these residues play a critical role in CaSR glycosylation and  
379 dimerization by forming intermolecular disulfide bonds (Fan, et al. 1997). Eight ADH1 mutations are  
380 located in the hinge region between lobes 1 and 2, and thirteen mutations affect residues within the  
381 homodimer interface (Figure 6E, Supplementary Table 1). Additionally, some of these mutations have  
382 been reported in more than one unrelated patient including Pro221Leu, reported in multiple independent  
383 cases (Supplementary Table 1). Studies of mutations affecting residues within the hinge region and  
384 homodimer interface have demonstrated these residues are important in the molecular connectivity  
385 between Ca<sup>2+</sup>-binding sites (Zhang, et al. 2014). Furthermore, many of these residues undergo  
386 movement from the CaSR inactive-to-active state and are located close to ligand-binding sites (Figure  
387 6E) (Geng et al. 2016; Zhang et al. 2016). It is therefore likely that these mutant residues elicit a gain-  
388 of-function by allowing conformational changes necessary for receptor activation to occur more readily  
389 than for wild-type receptor, by retaining the receptor in a partially active state that is fully activated at  
390 a lower concentration of ligand than wild-type receptor (Figure 6E) (Geng et al. 2016; Zhang et al.  
391 2014; Zhang et al. 2016). Consistent with such mutations favouring a partially active state, rather than  
392 enhancing protein levels or biasing signalling, when expressed *in vitro*, these mutant proteins do not

393 affect cell surface expression and enhance both  $\text{Ca}^{2+}_i$  and MAPK signalling (Gorvin, et al. 2018a; Silve,  
394 et al. 2005; Zhang et al. 2014).

395         Forty-one ADH1 mutations have been identified in the CaSR transmembrane domain and have  
396 provided important insights into CaSR activation (Figure 6F, Supplementary Table 1). More than 20 of  
397 these gain-of-function mutations are in the TM6-TM7 region, with 8 mutations identified in TM6, 10  
398 in TM7, and mutations in all four of the residues comprising ECL3 that tethers these two helices (Figure  
399 6F, Supplementary Table 1). Mutagenesis studies have shown that residues between Ile819 and Glu837,  
400 comprising the TM6-ECL3-TM7 region, participate in CaSR activation and are thus likely to be  
401 important for maintaining the receptor in its inactive conformation (Hu, et al. 2005). Moreover, studies  
402 of other class C GPCRs have shown the importance of TM6 in receptor activation and G-protein  
403 coupling (Binet et al. 2007; Xue et al. 2015). Finally, several positive allosteric modulators, bind to  
404 residues within this region, and are hypothesised to reduce the inhibitory constraints within the 7TMD  
405 to enhance sensitivity to  $\text{Ca}^{2+}_e$  (Hu et al. 2005). In contrast, negative allosteric modulators and FHH1  
406 mutants such as Pro823Ala, identified in this region, are hypothesised to impede rotation of TM6 (Hu  
407 et al. 2005). Thus, multiple studies provide evidence for the importance of TM6-ECL3-TM7 in CaSR  
408 activation. This understanding of the specific residues involved in CaSR activation could facilitate the  
409 rational design of allosteric modulators that are more likely to have an effect on receptor activity than  
410 by traditional compound screens.

411

#### 412 **Homozygous ADH1 mutations**

413         Two cases of ADH1 have been reported in which the patients had homozygous CaSR  
414 mutations. The first, a large deletion of Ser895 to Val1075 within the intracellular C-terminus  
415 (Lienhardt et al. 2000), was shown to increase  $\text{Ca}^{2+}_i$  responses and its possible effect on receptor  
416 degradation has been discussed in a previous section. The second mutation, Arg544Gln, was originally  
417 reported as a heterozygous mutation in an individual with FHH1 (Nissen, et al. 2012). However,  
418 subsequent identification of the mutation in the homozygous state with the opposite phenotype led the  
419 authors to perform a series of *in vitro* experiments assessing the effect of the mutation alone and in

420 combination with the wild-type receptor on both  $\text{Ca}^{2+}_i$  and MAPK signalling (Cavaco, et al. 2018). This  
421 revealed HEK293 cells expressing the Arg544Gln mutant construct had lower  $\text{EC}_{50}$  values compared  
422 to cells expressing either just the wild-type receptor, or equal amounts of wild-type and mutant receptor  
423 to mimic the heterozygous state (Cavaco et al. 2018). Thus, the mutation only affects CaSR signalling  
424 in the homozygous state, and in the heterozygous state is a benign variant. This is reflected in the public  
425 exome sequencing database, the Exome Aggregation Consortium (ExAc), which reports the  
426 heterozygous variant Arg544Gln in 96 unrelated individuals. Several other CaSR mutations have also  
427 been reported to be benign following functional testing (e.g. Thr14Ala) or due to their population  
428 frequency (e.g. Glu250Lys) (Hannan, et al. 2012; Pidasheva, et al. 2005). These findings highlight the  
429 importance of functionally investigating CaSR variants *in vitro* for the diagnosis of patients with  
430 calcaemic disorders.

431

#### 432 **ADH1 with Bartter's syndrome**

433 Occasionally, ADH1 patients have presented with features of Bartter's syndrome including  
434 hypokalaemia, hypomagnesaemia, metabolic alkalosis and hyperaldosteronaemia (Watanabe, et al.  
435 2002). Bartter's syndrome is a heterogenous disorder caused by defects in several proteins involved in  
436 transepithelial NaCl transport across the thick ascending limb of the loop of Henle (Hu, et al. 2002;  
437 Watanabe et al. 2002). To date, five CaSR mutations have been identified in association with ADH1  
438 and Bartter's syndrome and the clinical presentation and onset of Bartter's symptoms differ according  
439 to the type of mutation (Khorram, et al. 2015) (Supplementary Table 1). The Lys29Glu and Tyr829Cys  
440 mutations, are both associated with mild hypokalaemia and a late age of onset of 22 and 17 years,  
441 respectively (Khorram et al. 2015; Vezzoli, et al. 2006). Despite this, hypocalcaemia presents early and  
442 these patients develop signs of advanced hypocalcaemia including nephrocalcinosis and basal ganglia  
443 calcification. In contrast, patients with the Leu125Pro, Cys131Trp and Ala843Glu CaSR mutations  
444 present with a more severe form of Bartter's syndrome characterised by the full spectrum of symptoms  
445 including hypokalaemia, hypomagnesemia, metabolic alkalosis, hyperreninaemia and  
446 hyperaldosteronaemia in early childhood (Vargas-Poussou, et al. 2002). The Ala843Glu mutation is

447 associated with potent constitutive activity when examined *in vitro* by multiple assays (IP<sub>3</sub>, Ca<sup>2+</sup><sub>i</sub>  
448 mobilisation and ERK activation) (Leach et al. 2012; Watanabe et al. 2002). Consequently, when  
449 examined *in vitro*, increasing doses of Ca<sup>2+</sup><sub>e</sub> fail to activate the receptor as the calcium stores are rapidly  
450 depleted, and the E<sub>max</sub> is lower than in cells expressing wild-type CaSR (Leach et al. 2012). The Ala843  
451 residue is located within TM7 and the Glu843 mutation is hypothesised to lock the receptor in an active  
452 conformation, which is less susceptible to constraints caused by changes elsewhere in the TMD (Hu et  
453 al. 2005). Two CaSR residues, Leu125 and Cys131, located in loop 2 are mutated in both ADH1 and  
454 ADH1 with Bartter's syndrome. Mutation of the Leu125 residue to Pro125 causes ADH1 with Bartter's  
455 and is associated with a potent gain of functional activity in Ca<sup>2+</sup><sub>i</sub> response assays which may explain  
456 the severity of this patient's phenotype (Tan, et al. 2003). Mutation of this residue to Phe125, which  
457 causes ADH1, is associated with a severe hypocalcaemia (0.94 mmol/l), with an early age of onset at 4  
458 days old (Cole, et al. 2009), indicating this residue likely has an important role in receptor activation.  
459 Similarly, the one Cys131 mutation that is associated with both ADH1 and Bartter's syndrome, has a  
460 more potent effect on Ca<sup>2+</sup><sub>i</sub> signalling than other ADH1 mutations (Kinoshita, et al. 2014). The  
461 mechanism by which these mutations cause such a severe effect on receptor activity has still to be  
462 elucidated.

463

#### 464 ADH

- 465 • Is associated with more than 100 mutations, the majority of which are missense
- 466 • Most ADH patients have symptoms of hypocalcaemia (e.g. neuromuscular irritability) or  
467 associated features such as basal ganglia calcification or nephrocalcinosis
- 468 • The ECD missense mutations are clustered in three key sites: loop 2; the hinge region between  
469 lobes 1 and 2; and the homodimer interface
- 470 • TMD mutations are clustered in TM6-ECL3-TM7
- 471 • Occasionally ADH1 can be associated with a Bartter's syndrome phenotype

472

## 473 **CaSR residues harbouring both inactivating and activating mutations**

474 Twelve residues have been identified that are the location of both germline loss- and gain-of-  
475 function mutations that cause FHH1 and ADH1, respectively (Supplementary Table 1). Such residues  
476 have previously been termed ‘switch’ residues as they are thought to be important in switching the  
477 receptor from the inactive to active state and may direct CaSR signalling via the  $Ca^{2+}_i$  or MAPK  
478 pathways (Gorvin et al. 2018a; Stoy and Gurevich 2015; Zhang et al. 2014). Such switch mutations are  
479 not unique to CaSR and have been observed in other GPCRs including the human arginine vasopressin  
480 receptor (Stoy and Gurevich 2015). Structural studies comparing the active and inactive states of CaSR  
481 has demonstrated these residues are often located in regions that undergo large conformational changes  
482 upon ligand-binding consistent with studies of other GPCRs (Gorvin et al. 2018a; Stoy and Gurevich  
483 2015). Six of the CaSR switch residues are located in critical regions within the VFTD, including the  
484 dimer interface close to loop 1 (Val104), at the lobe 1-lobe 2 hinge region (Leu173, Asn178, Pro221),  
485 and within the ligand-binding site at the hinge region (Glu297) (Geng et al. 2016; Gorvin et al. 2018a).  
486 The other five switch residues are located in the TMD clustered around TM3 and TM6, which structural  
487 studies of other class C GPCRs have revealed undergo substantial outward movement during receptor  
488 activation to accommodate G-protein coupling (Binet et al. 2007; Leach et al. 2012; Xue et al. 2015).

489 However, designating all residues with both inactivating and activating mutations as switch  
490 residues may be too simplistic given the range of molecular phenotypes that render a receptor as active  
491 or inactive. For example, a loss-of-function mutation may arise by several mechanisms including  
492 reduced cell surface expression (e.g. due to ER retention), impaired GPCR-G-protein coupling or  
493 reduced ligand binding. As such, detailed molecular profiling of each mutation may be required to  
494 determine if a residue can be designated a switch residue. Eleven of the 12 CaSR residues described  
495 with shared inactivating and activating mutations have been functionally characterised. The FHH1-  
496 associated mutations in six of these residues (Glu297, Ser657, Arg680, Met734, Asn802 and Ser820)  
497 have reduced cell surface expression in at least one study, which is likely to cause, or contribute to, the  
498 reduction in CaSR signal transduction (Bai et al. 1996; Gorvin et al. 2018a; Leach et al. 2012). Most of  
499 these residues are located within the TMD and mutations in these residues may affect the ability of the

500 receptor to fold efficiently and traffic to the cell surface, thus reducing the receptors exposure to agonist  
501 (Leach et al. 2012). Indeed, 17 TMD mutations reported to cause FHH1 reduce cell surface expression  
502 in at least one study (Supplementary Table 1). However, while this is true of some mutations  
503 (Met734Arg), the intrinsic signalling capacity of other mutant CaSR proteins (Arg680Cys, Arg680His)  
504 has been shown to be retained, while others may have a gain-of-function but with reduced expression  
505 (Ser657Tyr) (Leach et al. 2012). Therefore, it is unlikely that all of these mutations impair structural  
506 integrity of the receptors, and there must be another reason that cell surface expression is impaired, with  
507 reduced ability to form higher-order oligomers suggested as one possible contributor (Leach et al.  
508 2012).

509

### 510 **Biased signalling**

511 Biased signalling is the propensity of distinct receptor conformations to preferentially couple to specific  
512 signalling pathways. As such, promiscuous receptors such as the CaSR that can bind multiple ligands  
513 and couple to several G-protein subtypes, can exhibit distinct profiles for different agonists (Thomsen,  
514 et al. 2012). In HEK293 cells when stimulated with  $\text{Ca}^{2+}_e$ , the CaSR preferentially couples to activate  
515  $\text{IP}_3$  and inhibit cAMP production, rather than phosphorylation of ERK1/2 (i.e. MAPK signalling)  
516 (Thomsen et al. 2012). In contrast, disease-causing CASR mutants located in the TMD or switch  
517 residues, have been shown to switch this preferential signalling by stabilising receptor conformations  
518 that couple differentially to intracellular signalling pathways (Gorvin et al. 2018a; Gorvin, et al. 2018b;  
519 Leach et al. 2012). Many ADH1 mutants couple more strongly to  $\text{Ca}^{2+}_i$ ; while inactivating mutations  
520 signal equally via the  $\text{Ca}^{2+}_i$  and MAPK pathways, or predominantly via MAPK pathways (Leach et al.  
521 2012). There are exceptions to this including the constitutively active Ala843Glu mutant, which  
522 enhances basal activity of both  $\text{Ca}^{2+}_i$  and MAPK pathways (Leach et al. 2012; Watanabe et al. 2002).  
523 Additionally, an ADH1-associated mutant, Arg680Gly, was recently described that enhanced MAPK  
524 signalling by disrupting a transmembrane salt bridge to activate a  $\beta$ -arrestin-mediated pathway (Gorvin  
525 et al. 2018b). Discerning the distinct signalling profiles of some CaSR mutations that cause

526 symptomatic hyper/hypocalcaemia may be pertinent to the rational design of drugs to selectively  
527 regulate distinct signalling pathway (Leach, et al. 2014; Leach et al. 2012).

528

## 529 **Future directions**

530 As increasingly more population level genetic data becomes available through datasets such as ExAc  
531 and The 100,000 Genomes Project, and with whole-exome/ whole-genome sequencing used more  
532 frequently in patient diagnoses, it is likely that many more CaSR variants of unknown significance on  
533 patient health will be identified. How to approach such variants is a frequent problem, especially as  
534 pathogenicity prediction programs are often incorrect, and as our understanding of receptor signalling  
535 becomes increasingly more complex. An understanding of individual residue's roles in receptor  
536 structure and activation mechanisms, combined with high-throughput, reliable functional assays, could  
537 provide additional information to allow clinician's to make more informed decisions about the  
538 likelihood of variant pathogenicity. It is likely that in future more interactions between clinicians,  
539 geneticists and researchers will be required to understand how these variants impact receptor function  
540 and human health.

541 In the last decade, the genetic heterogeneity of FHH and ADH has emerged, with mutations in the  $G\alpha 11$   
542 protein, by which CaSR signals, and the adaptor protein-2 sigma subunit ( $AP2\sigma$ ), by which CaSR is  
543 internalized, revealed as additional contributors to calcaemic disorders. Studies of these mutations have  
544 uncovered novel mechanisms by which CaSR is internalised, and demonstrated that CaSR can signal  
545 by an endosomal pathway (Gorvin, et al. 2018a). Moreover, some FHH and ADH patients do not have  
546 mutations in any of these three genes and discovery of the mutant proteins in these cases is likely to  
547 yield further insights into CaSR signalling and trafficking. Understanding the mechanisms by which  
548 these novel signal pathways arise, and how receptor mutations affect these pathways are likely to  
549 provide continued insights into the CaSR for years to come.

550

551

552 **Declaration of interest:** The author has no conflict of interest.

553

554 **Funding:** This research did not receive any specific grant from any funding agency in the public,  
555 commercial or not-for-profit sector.

556

557 **References**

- 558 Bai M, Quinn S, Trivedi S, Kifor O, Pearce SH, Pollak MR, Krapcho K, Hebert SC & Brown EM 1996  
559 Expression and characterization of inactivating and activating mutations in the human Ca<sup>2+</sup>-sensing  
560 receptor. *J Biol Chem* **271** 19537-19545.
- 561 Bai M, Trivedi S, Lane CR, Yang Y, Quinn SJ & Brown EM 1998 Protein kinase C phosphorylation of  
562 threonine at position 888 in Ca<sup>2+</sup>-sensing receptor (CaR) inhibits coupling to Ca<sup>2+</sup> store release. *J*  
563 *Biol Chem* **273** 21267-21275.
- 564 Binet V, Duthey B, Lecaillon J, Vol C, Quoyer J, Labesse G, Pin JP & Prezeau L 2007 Common  
565 structural requirements for heptahelical domain function in class A and class C G protein-coupled  
566 receptors. *J Biol Chem* **282** 12154-12163.
- 567 Brown EM, Gamba G, Riccardi D, Lombardi M, Butters R, Kifor O, Sun A, Hediger MA, Lytton J &  
568 Hebert SC 1993 Cloning and characterization of an extracellular Ca(2+)-sensing receptor from bovine  
569 parathyroid. *Nature* **366** 575-580.
- 570 Cavaco BM, Canaff L, Nolin-Lapalme A, Vieira M, Silva TN, Saramago A, Domingues R, Rutter MM,  
571 Hudon J, Gleason JL, et al. 2018 Homozygous Calcium-Sensing Receptor Polymorphism R544Q  
572 Presents as Hypocalcemic Hypoparathyroidism. *J Clin Endocrinol Metab* **103** 2879-2888.
- 573 Chikatsu N, Fukumoto S, Suzawa M, Tanaka Y, Takeuchi Y, Takeda S, Tamura Y, Matsumoto T &  
574 Fujita T 1999 An adult patient with severe hypercalcaemia and hypocalciuria due to a novel  
575 homozygous inactivating mutation of calcium-sensing receptor. *Clin Endocrinol (Oxf)* **50** 537-543.
- 576 Christensen SE, Nissen PH, Vestergaard P, Heickendorff L, Brixen K & Mosekilde L 2008  
577 Discriminative power of three indices of renal calcium excretion for the distinction between familial  
578 hypocalciuric hypercalcaemia and primary hyperparathyroidism: a follow-up study on methods. *Clin*  
579 *Endocrinol (Oxf)* **69** 713-720.
- 580 Cole DE, Yun FH, Wong BY, Shuen AY, Booth RA, Scillitani A, Pidasheva S, Zhou X, Canaff L &  
581 Hendy GN 2009 Calcium-sensing receptor mutations and denaturing high performance liquid  
582 chromatography. *J Mol Endocrinol* **42** 331-339.
- 583 Conigrave AD 2016 The Calcium-Sensing Receptor and the Parathyroid: Past, Present, Future. *Front*  
584 *Physiol* **7** 563.
- 585 Dong B, Endo I, Ohnishi Y, Kondo T, Hasegawa T, Amizuka N, Kiyonari H, Shioi G, Abe M,  
586 Fukumoto S, et al. 2015 Calcilytic Ameliorates Abnormalities of Mutant Calcium-Sensing Receptor  
587 (CaSR) Knock-In Mice Mimicking Autosomal Dominant Hypocalcemia (ADH). *J Bone Miner Res* **30**  
588 1980-1993.
- 589 Dore AS, Okrasa K, Patel JC, Serrano-Vega M, Bennett K, Cooke RM, Errey JC, Jazayeri A, Khan S,  
590 Tehan B, et al. 2014 Structure of class C GPCR metabotropic glutamate receptor 5 transmembrane  
591 domain. *Nature* **511** 557-562.
- 592 Eastell R, Brandi ML, Costa AG, D'Amour P, Shoback DM & Thakker RV 2014 Diagnosis of  
593 asymptomatic primary hyperparathyroidism: proceedings of the Fourth International Workshop. *J Clin*  
594 *Endocrinol Metab* **99** 3570-3579.
- 595 Fan G, Goldsmith PK, Collins R, Dunn CK, Krapcho KJ, Rogers KV & Spiegel AM 1997 N-linked  
596 glycosylation of the human Ca<sup>2+</sup> receptor is essential for its expression at the cell surface.  
597 *Endocrinology* **138** 1916-1922.
- 598 Geng Y, Mosyak L, Kurinov I, Zuo H, Sturchler E, Cheng TC, Subramanyam P, Brown AP, Brennan  
599 SC, Mun HC, et al. 2016 Structural mechanism of ligand activation in human calcium-sensing receptor.  
600 *Elife* **5**.
- 601 Gorvin CM, Frost M, Malinauskas T, Cranston T, Boon H, Siebold C, Jones EY, Hannan FM & Thakker  
602 RV 2018a Calcium-sensing receptor residues with loss- and gain-of-function mutations are located in  
603 regions of conformational change and cause signalling bias. *Hum Mol Genet* **27** 3720-3733.
- 604 Gorvin CM, Hannan FM, Cranston T, Valta H, Makitie O, Schalin-Jantti C & Thakker RV 2018b  
605 Cinacalcet Rectifies Hypercalcaemia in a Patient With Familial Hypocalciuric Hypercalcaemia Type 2  
606 (FHH2) Caused by a Germline Loss-of-Function Galpha11 Mutation. *J Bone Miner Res* **33** 32-41.
- 607 Gorvin CM, Rogers A, Hastoy B, Tarasov AI, Frost M, Sposini S, Inoue A, Whyte MP, Rorsman P,  
608 Hanyaloglu AC, et al. 2018a AP2sigma Mutations Impair Calcium-Sensing Receptor Trafficking and

609 Signaling, and Show an Endosomal Pathway to Spatially Direct G-Protein Selectivity. *Cell Rep* **22**  
610 1054-1066.

611 Hannan FM, Nesbit MA, Christie PT, Lissens W, Van der Schueren B, Bex M, Bouillon R & Thakker  
612 RV 2010 A homozygous inactivating calcium-sensing receptor mutation, Pro339Thr, is associated with  
613 isolated primary hyperparathyroidism: correlation between location of mutations and severity of  
614 hypercalcaemia. *Clin Endocrinol (Oxf)* **73** 715-722.

615 Hannan FM, Nesbit MA, Zhang C, Cranston T, Curley AJ, Harding B, Fratter C, Rust N, Christie PT,  
616 Turner JJ, et al. 2012 Identification of 70 calcium-sensing receptor mutations in hyper- and hypo-  
617 calcaemic patients: evidence for clustering of extracellular domain mutations at calcium-binding sites.  
618 *Hum Mol Genet* **21** 2768-2778.

619 Hannan FM & Thakker RV 2013 Calcium-sensing receptor (CaSR) mutations and disorders of calcium,  
620 electrolyte and water metabolism. *Best Pract Res Clin Endocrinol Metab* **27** 359-371.

621 Ho C, Conner DA, Pollak MR, Ladd DJ, Kifor O, Warren HB, Brown EM, Seidman JG & Seidman CE  
622 1995 A mouse model of human familial hypocalciuric hypercalcemia and neonatal severe  
623 hyperparathyroidism. *Nat Genet* **11** 389-394.

624 Hu J, McLarnon SJ, Mora S, Jiang J, Thomas C, Jacobson KA & Spiegel AM 2005 A region in the  
625 seven-transmembrane domain of the human Ca<sup>2+</sup> receptor critical for response to Ca<sup>2+</sup>. *J Biol Chem*  
626 **280** 5113-5120.

627 Hu J, Mora S, Colussi G, Proverbio MC, Jones KA, Bolzoni L, De Ferrari ME, Civati G & Spiegel AM  
628 2002 Autosomal dominant hypocalcemia caused by a novel mutation in the loop 2 region of the human  
629 calcium receptor extracellular domain. *J Bone Miner Res* **17** 1461-1469.

630 Huang Y & Breitwieser GE 2007 Rescue of calcium-sensing receptor mutants by allosteric modulators  
631 reveals a conformational checkpoint in receptor biogenesis. *J Biol Chem* **282** 9517-9525.

632 Huang Y, Niwa J, Sobue G & Breitwieser GE 2006 Calcium-sensing receptor ubiquitination and  
633 degradation mediated by the E3 ubiquitin ligase dorfins. *J Biol Chem* **281** 11610-11617.

634 Huang Y, Zhou Y, Wong HC, Castiblanco A, Chen Y, Brown EM & Yang JJ 2010 Calmodulin  
635 regulates Ca<sup>2+</sup>-sensing receptor-mediated Ca<sup>2+</sup> signaling and its cell surface expression. *J Biol Chem*  
636 **285** 35919-35931.

637 Khorram D, Choi M, Roos BR, Stone EM, Kopel T, Allen R, Alward WL, Scheetz TE & Fingert JH  
638 2015 Novel TMEM98 mutations in pedigrees with autosomal dominant nanophthalmos. *Mol Vis* **21**  
639 1017-1023.

640 Kinoshita Y, Hori M, Taguchi M, Watanabe S & Fukumoto S 2014 Functional activities of mutant  
641 calcium-sensing receptors determine clinical presentations in patients with autosomal dominant  
642 hypocalcemia. *J Clin Endocrinol Metab* **99** E363-368.

643 Lazarus S, Pretorius CJ, Khafagi F, Campion KL, Brennan SC, Conigrave AD, Brown EM & Ward DT  
644 2011 A novel mutation of the primary protein kinase C phosphorylation site in the calcium-sensing  
645 receptor causes autosomal dominant hypocalcemia. *Eur J Endocrinol* **164** 429-435.

646 Leach K, Sexton PM, Christopoulos A & Conigrave AD 2014 Engendering biased signalling from the  
647 calcium-sensing receptor for the pharmacotherapy of diverse disorders. *Br J Pharmacol* **171** 1142-1155.

648 Leach K, Wen A, Davey AE, Sexton PM, Conigrave AD & Christopoulos A 2012 Identification of  
649 molecular phenotypes and biased signaling induced by naturally occurring mutations of the human  
650 calcium-sensing receptor. *Endocrinology* **153** 4304-4316.

651 Lienhardt A, Garabedian M, Bai M, Sinding C, Zhang Z, Lagarde JP, Boulesteix J, Rigaud M, Brown  
652 EM & Kottler ML 2000 A large homozygous or heterozygous in-frame deletion within the calcium-  
653 sensing receptor's carboxylterminal cytoplasmic tail that causes autosomal dominant hypocalcemia. *J*  
654 *Clin Endocrinol Metab* **85** 1695-1702.

655 Maruca K, Brambilla I, Mingione A, Bassi L, Capelli S, Brasacchio C, Soldati L, Cisternino M & Mora  
656 S 2017 Autosomal dominant hypocalcemia due to a truncation in the C-tail of the calcium-sensing  
657 receptor. *Mol Cell Endocrinol* **439** 187-193.

658 Marx SJ 2018 Familial Hypocalciuric Hypercalcemia as an Atypical Form of Primary  
659 Hyperparathyroidism. *J Bone Miner Res* **33** 27-31.

660 Mayr B, Schnabel D, Dorr HG & Schofl C 2016 GENETICS IN ENDOCRINOLOGY: Gain and loss  
661 of function mutations of the calcium-sensing receptor and associated proteins: current treatment  
662 concepts. *Eur J Endocrinol* **174** R189-208.

663 McCullough J, Clague MJ & Urbe S 2004 AMSH is an endosome-associated ubiquitin isopeptidase. *J*  
664 *Cell Biol* **166** 487-492.

665 Nemeth EF & Scarpa A 1987 Rapid mobilization of cellular Ca<sup>2+</sup> in bovine parathyroid cells evoked  
666 by extracellular divalent cations. Evidence for a cell surface calcium receptor. *J Biol Chem* **262** 5188-  
667 5196.

668 Nissen PH, Christensen SE, Ladefoged SA, Brixen K, Heickendorff L & Mosekilde L 2012  
669 Identification of rare and frequent variants of the CASR gene by high-resolution melting. *Clin Chim*  
670 *Acta* **413** 605-611.

671 Nyweide K, Feldman KW, Gunther DF, Done S, Lewis C & Van Eenwyk C 2006 Hypocalciuric  
672 hypercalcemia presenting as neonatal rib fractures: a newly described mutation of the calcium-sensing  
673 receptor gene. *Pediatr Emerg Care* **22** 722-724.

674 Obermannova B, Sumnik Z, Dusatkova P, Cinek O, Grant M, Lebl J & Hendy GN 2016 Novel calcium-  
675 sensing receptor cytoplasmic tail deletion mutation causing autosomal dominant hypocalcemia:  
676 molecular and clinical study. *Eur J Endocrinol* **174** K1-K11.

677 Pidasheva S, Canaff L, Simonds WF, Marx SJ & Hendy GN 2005 Impaired cotranslational processing  
678 of the calcium-sensing receptor due to signal peptide missense mutations in familial hypocalciuric  
679 hypercalcemia. *Hum Mol Genet* **14** 1679-1690.

680 Pollak MR, Brown EM, Chou YH, Hebert SC, Marx SJ, Steinmann B, Levi T, Seidman CE & Seidman  
681 JG 1993 Mutations in the human Ca(2+)-sensing receptor gene cause familial hypocalciuric  
682 hypercalcemia and neonatal severe hyperparathyroidism. *Cell* **75** 1297-1303.

683 Pollak MR, Chou YH, Marx SJ, Steinmann B, Cole DE, Brandi ML, Papapoulos SE, Menko FH, Hendy  
684 GN, Brown EM, et al. 1994 Familial hypocalciuric hypercalcemia and neonatal severe  
685 hyperparathyroidism. Effects of mutant gene dosage on phenotype. *J Clin Invest* **93** 1108-1112.

686 Raue F, Pichl J, Dorr HG, Schnabel D, Heidemann P, Hammersen G, Jaursch-Hancke C, Santen R,  
687 Schofl C, Wabitsch M, et al. 2011 Activating mutations in the calcium-sensing receptor: genetic and  
688 clinical spectrum in 25 patients with autosomal dominant hypocalcaemia - a German survey. *Clin*  
689 *Endocrinol (Oxf)* **75** 760-765.

690 Reh CM, Hendy GN, Cole DE & Jeandron DD 2011 Neonatal hyperparathyroidism with a heterozygous  
691 calcium-sensing receptor (CASR) R185Q mutation: clinical benefit from cinacalcet. *J Clin Endocrinol*  
692 *Metab* **96** E707-712.

693 Roszko KL, Bi RD & Mannstadt M 2016 Autosomal Dominant Hypocalcemia (Hypoparathyroidism)  
694 Types 1 and 2. *Front Physiol* **7** 458.

695 Shoback DM, Membreno LA & McGhee JG 1988 High calcium and other divalent cations increase  
696 inositol trisphosphate in bovine parathyroid cells. *Endocrinology* **123** 382-389.

697 Silve C, Petrel C, Leroy C, Bruel H, Mallet E, Rognan D & Ruat M 2005 Delineating a Ca<sup>2+</sup> binding  
698 pocket within the venus flytrap module of the human calcium-sensing receptor. *J Biol Chem* **280** 37917-  
699 37923.

700 Stoy H & Gurevich VV 2015 How genetic errors in GPCRs affect their function: Possible therapeutic  
701 strategies. *Genes Dis* **2** 108-132.

702 Sun X, Huang L, Wu J, Tao Y & Yang F 2018 Novel homozygous inactivating mutation of the calcium-  
703 sensing receptor gene in neonatal severe hyperparathyroidism responding to cinacalcet therapy: A case  
704 report and literature review. *Medicine (Baltimore)* **97** e13128.

705 Taki K, Kogai T, Sakumoto J, Namatame T & Hishinuma A 2015 Familial hypocalciuric hypercalcemia  
706 with a de novo heterozygous mutation of calcium-sensing receptor. *Endocrinol Diabetes Metab Case*  
707 *Rep* **2015** 150016.

708 Tan YM, Cardinal J, Franks AH, Mun HC, Lewis N, Harris LB, Prins JB & Conigrave AD 2003  
709 Autosomal dominant hypocalcemia: a novel activating mutation (E604K) in the cysteine-rich domain  
710 of the calcium-sensing receptor. *J Clin Endocrinol Metab* **88** 605-610.

711 Thomsen AR, Hvidtfeldt M & Brauner-Osborne H 2012 Biased agonism of the calcium-sensing  
712 receptor. *Cell Calcium* **51** 107-116.

713 Toke J, Czirjak G, Patocs A, Enyedi B, Gergics P, Csakvary V, Enyedi P & Toth M 2007 Neonatal  
714 severe hyperparathyroidism associated with a novel de novo heterozygous R551K inactivating mutation  
715 and a heterozygous A986S polymorphism of the calcium-sensing receptor gene. *Clin Endocrinol (Oxf)*  
716 **67** 385-392.

717 Vargas-Poussou R, Huang C, Hulin P, Houillier P, Jeunemaitre X, Paillard M, Planelles G, Dechaux  
718 M, Miller RT & Antignac C 2002 Functional characterization of a calcium-sensing receptor mutation  
719 in severe autosomal dominant hypocalcemia with a Bartter-like syndrome. *J Am Soc Nephrol* **13** 2259-  
720 2266.

721 Vezzoli G, Arcidiacono T, Paloschi V, Terranegra A, Biasion R, Weber G, Mora S, Syren ML, Coviello  
722 D, Cusi D, et al. 2006 Autosomal dominant hypocalcemia with mild type 5 Bartter syndrome. *J Nephrol*  
723 **19** 525-528.

724 Watanabe S, Fukumoto S, Chang H, Takeuchi Y, Hasegawa Y, Okazaki R, Chikatsu N & Fujita T 2002  
725 Association between activating mutations of calcium-sensing receptor and Bartter's syndrome. *Lancet*  
726 **360** 692-694.

727 White E, McKenna J, Cavanaugh A & Breitwieser GE 2009 Pharmacochaperone-mediated rescue of  
728 calcium-sensing receptor loss-of-function mutants. *Mol Endocrinol* **23** 1115-1123.

729 Wystrychowski A, Pidasheva S, Canaff L, Chudek J, Kokot F, Wiecek A & Hendy GN 2005 Functional  
730 characterization of calcium-sensing receptor codon 227 mutations presenting as either familial (benign)  
731 hypocalciuric hypercalcemia or neonatal hyperparathyroidism. *J Clin Endocrinol Metab* **90** 864-870.

732 Xue L, Rovira X, Scholler P, Zhao H, Liu J, Pin JP & Rondard P 2015 Major ligand-induced  
733 rearrangement of the heptahelical domain interface in a GPCR dimer. *Nat Chem Biol* **11** 134-140.

734 Zhang C, Mulpuri N, Hannan FM, Nesbit MA, Thakker RV, Hamelberg D, Brown EM & Yang JJ 2014  
735 Role of Ca<sup>2+</sup> and L-Phe in regulating functional cooperativity of disease-associated "toggle" calcium-  
736 sensing receptor mutations. *PLoS One* **9** e113622.

737 Zhang C, Zhang T, Zou J, Miller CL, Gorkhali R, Yang JY, Schillmiller A, Wang S, Huang K, Brown  
738 EM, et al. 2016 Structural basis for regulation of human calcium-sensing receptor by magnesium ions  
739 and an unexpected tryptophan derivative co-agonist. *Sci Adv* **2** e1600241.

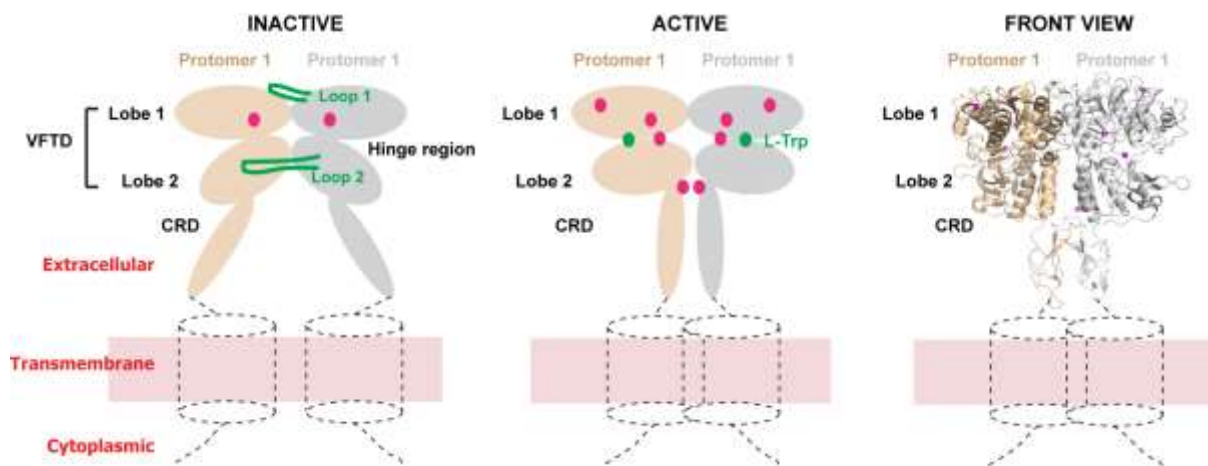
740 Zhang M & Breitwieser GE 2005 High affinity interaction with filamin A protects against calcium-  
741 sensing receptor degradation. *J Biol Chem* **280** 11140-11146.

742

743 **FIGURE 1**

744 Schematic diagram showing the structure and activation mechanism of CaSR. All panels focus on the  
745 ECD as two crystal structures of this region have been published (Geng et al. 2016; Zhang et al. 2016).  
746 The TMD and ICD are shown by hatched outline to depict where these regions are positioned. The left  
747 and middle images show the inactive and active states in cartoon form, and the image to the right, the  
748 crystal structure of the ECD in front view, on which the cartoons are based (PDB:5K5S) (Geng et al.  
749 2016). The receptor exists primarily at cell surfaces as a homodimer and each protomer ECD comprises  
750 a bi-lobed venus flytrap domain (VFTD) and a cysteine-rich domain (CRD). In the inactive state,  
751 homodimer interactions occur predominantly at the lobe 1-lobe 1 interface and at loop 1 and 2. On  
752 receptor activation, each protomer undergoes a 29° rotation, bringing the Lobe 2-Lobe 2 and CRD-  
753 CRD domains into closer proximity, and expanding the homodimer interface. Pink spheres show Ca<sup>2+</sup>-  
754 binding sites and green spheres L-Trp binding sites. Loops 1 and 2 are only shown on the inactive  
755 cartoon.

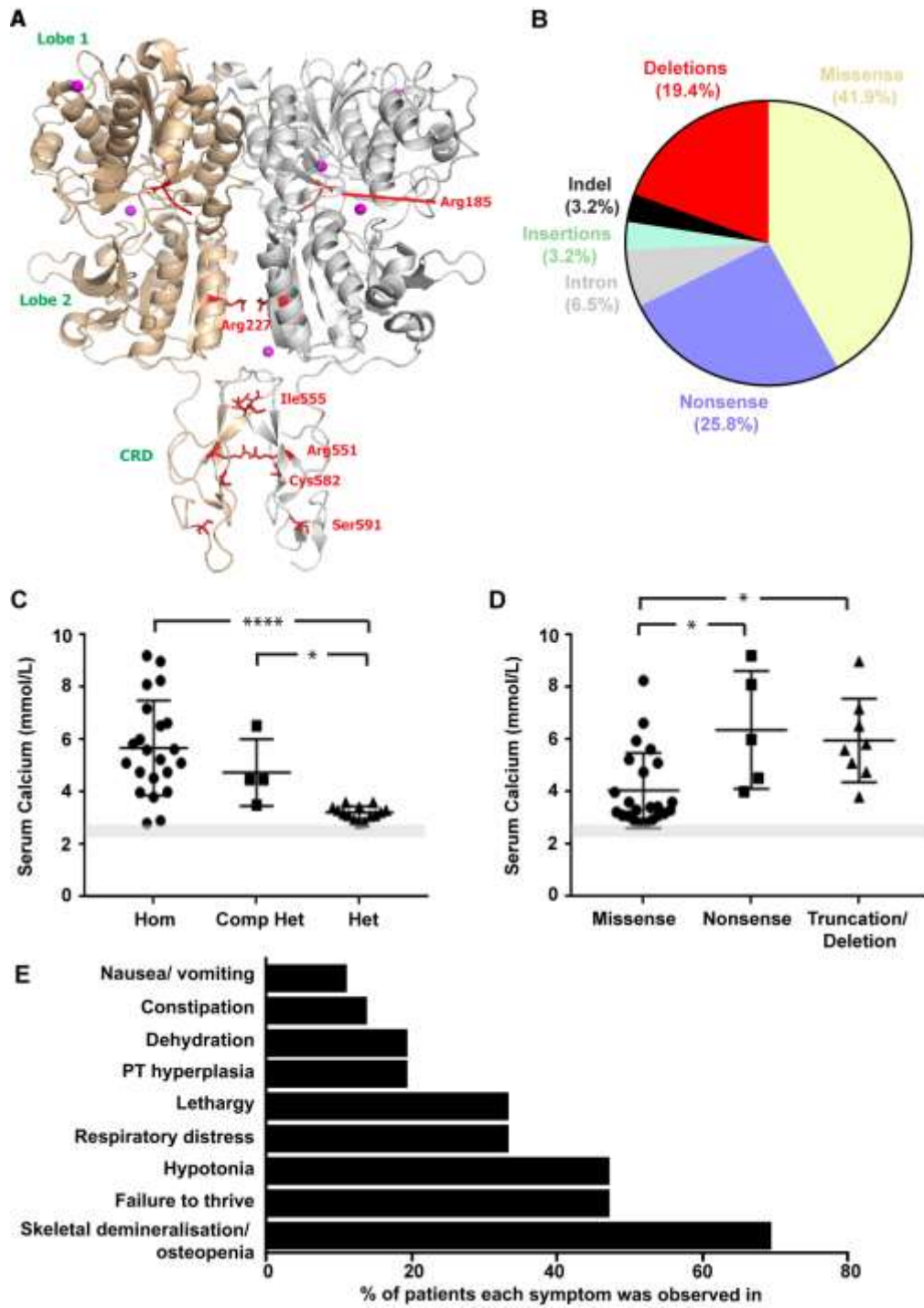
756



757

758 **FIGURE 2**

759 (A) Model showing locations of NSHPT-associated heterozygous mutations (red sticks) on the active  
760 structure of the CaSR-ECD (PDB:5K5S) (Geng et al. 2016). The six heterozygous mutations are located  
761 within domain interfaces that are critical for receptor activation. (B) Pie chart showing type of mutations  
762 described in NSHPT patients expressed as a percentage. Only the homozygous mutations are shown.  
763 The nonsense and deletion mutations lead to partial or complete loss of the TMD and C-terminus in  
764 NSHPT. Indel, insertion/deletion. (C) Serum calcium values of patients based on inheritance patterns  
765 of mutant alleles. Serum calcium concentrations are higher in homozygous and compound heterozygous  
766 patients indicating a gene dosage effect. The grey line indicates the normal range values (2.2-2.6  
767 mmol/L). (D) Serum calcium values of patients based on type of mutation showing nonsense and  
768 truncation mutations are associated with increased serum calcium values compared to missense  
769 mutations. There is no significant difference between serum calcium values in patients with nonsense  
770 or truncation mutations. (E) Percentage of NSHPT patients each symptom was observed in. All analyses  
771 are based on published biochemistry and clinical descriptions of NSHPT mutations from 41 patients  
772 (Supplementary Table 1). Statistical analyses were performed by one-way ANOVA. \*\*\*\*p<0.0001,  
773 \*p<0.01.

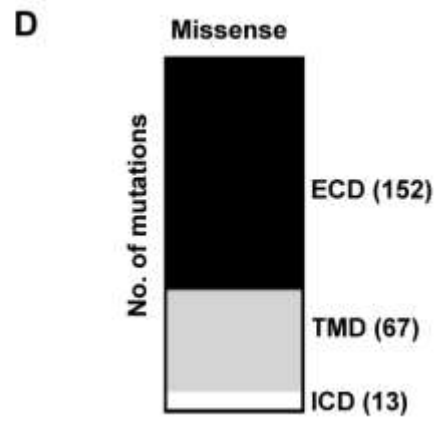
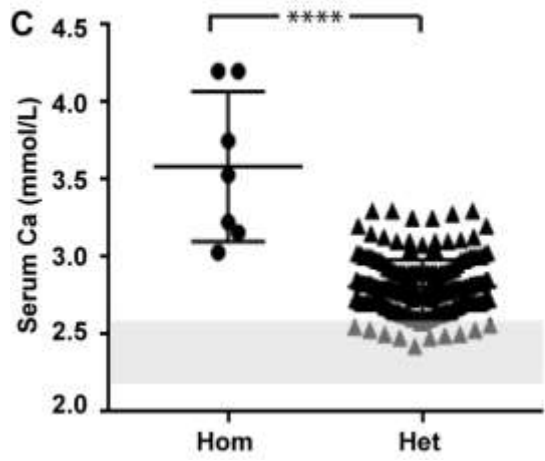
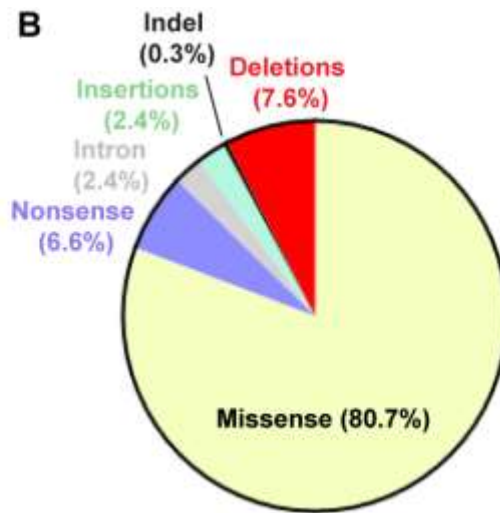
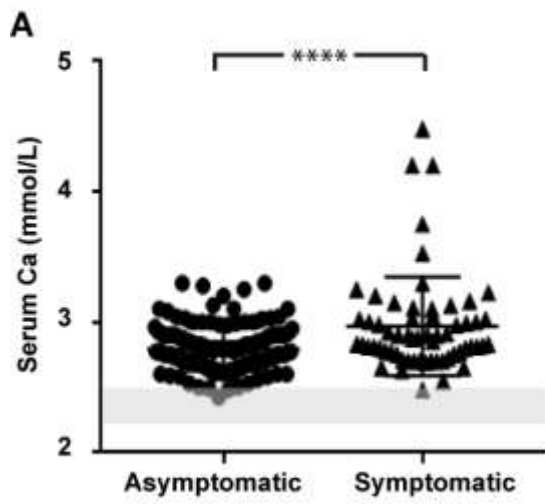


774

775

776 **FIGURE 3**

777 Genetic landscape of FHH1 mutations. (A) Mean serum calcium values of FHH1 patients with  
778 asymptomatic vs. symptomatic hypercalcaemia. Patients were regarded as symptomatic if they  
779 presented with typical signs of hypercalcaemia (e.g. headaches, fatigue, muscle cramps, constipation,  
780 nausea and vomiting) or associated phenotypes (e.g. nephrocalcinosis/nephrolithiasis, osteoporosis  
781 and/or fractures, pancreatitis). Patients with symptomatic hypercalcaemia had higher serum calcium  
782 values than asymptomatic individuals. Grey line indicates normal range values (2.2-2.6 mmol/L). (B)  
783 **Pie chart showing type of mutations described in FHH1 patients expressed as a percentage.** Percentage  
784 of FHH1 patients with different types of mutation. Approximately 80% of FHH1 mutations are  
785 missense. (C) The majority of FHH1 mutations are heterozygous and these patients have milder  
786 hypercalcaemia than those with homozygous mutations. (D) Number of FHH1 mutations located in  
787 each domain of the CaSR. All analyses are based on published biochemistry and descriptions of FHH1  
788 mutations from 290 individuals/kindreds (Supplementary Table 1). Statistical analyses were performed  
789 by Student's t-test. \*\*\*\*p<0.0001.

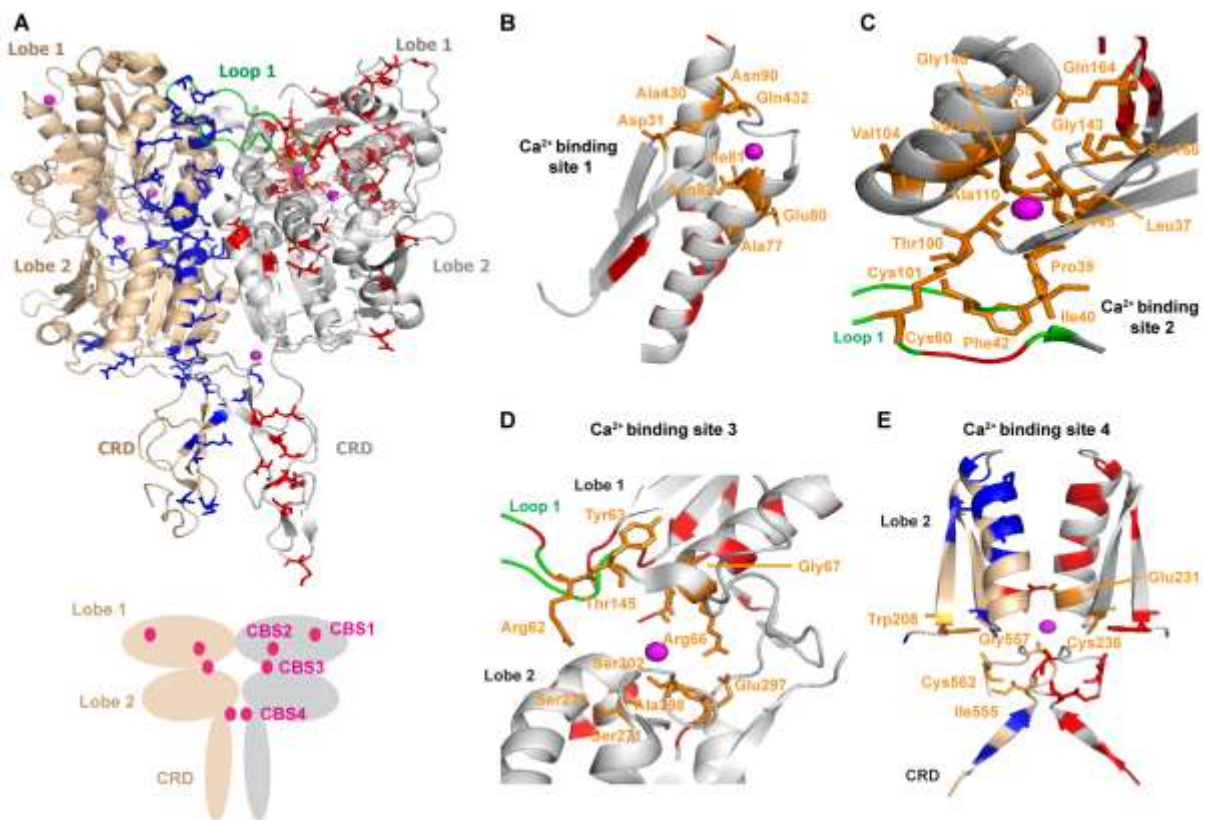


790

791

792 **FIGURE 4**

793 Clustering of FHH1 mutations at dimer interfaces and ligand-binding sites. (A) Top: model showing  
 794 the locations of the FHH1-associated mutations in the active structure of the CaSR-ECD (PDB:5K5S)  
 795 (Geng et al. 2016). Mutations shown in blue are located in domain interfaces including the lobe 1-lobe  
 796 2 hinge region, the CRD-CRD interface and the homodimers interface. FHH1 mutations are also located  
 797 within loop 1 (green) which extends from one protomer across the homodimer interface to interact with  
 798 the other protomer. The mutations shown in red are the other residues mutated by missense FHH1  
 799 mutations. Several of these mutations are located close to Ca<sup>2+</sup>-binding sites (shown as magenta  
 800 spheres). Bottom: cartoon of the active CaSR showing locations of Ca<sup>2+</sup>-binding sites (CBS1-4). (B-D)  
 801 CaSR residues that are mutated in FHH1 and are located within 10Å of each of the four Ca<sup>2+</sup>-binding  
 802 sites shown in orange. Mutations at these residues could affect ligand binding to the CaSR and receptor  
 803 activation. Surrounding residues that are mutated in FHH1 and located >10Å from the Ca<sup>2+</sup>-binding  
 804 sites are shown in red or blue without sticks.

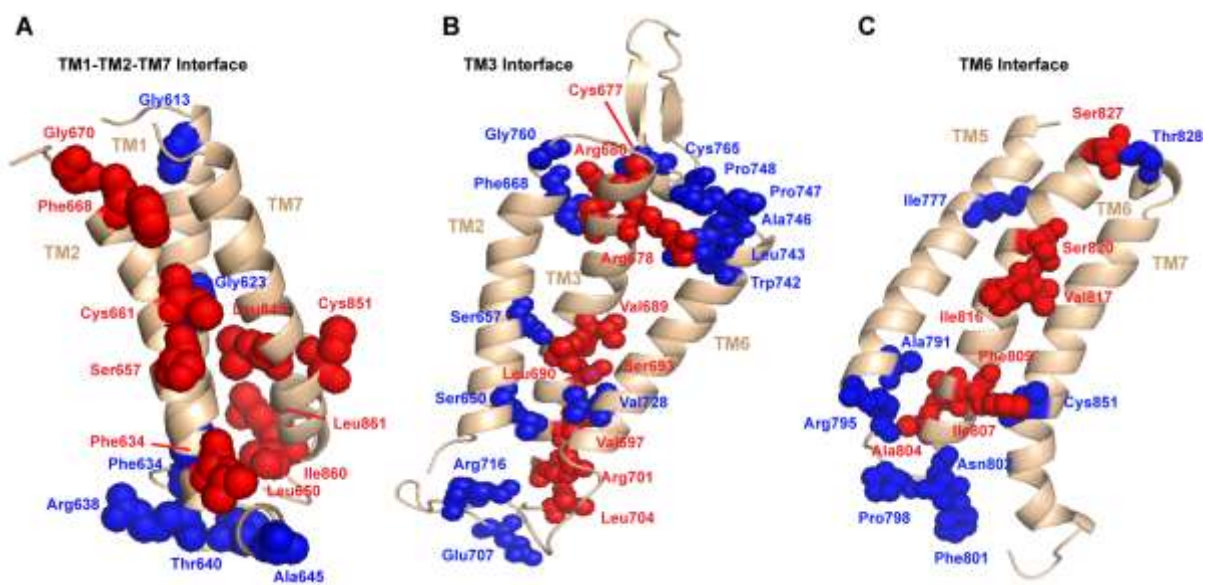


805

806 **FIGURE 5**

807 FHH1 mutations located in the TMD. Homology model of the CaSR-TMD based on the crystal structure  
808 of mGluR5 (PDB:4OO9) (Dore et al. 2014). FHH1 mutations (shown as red or blue spheres) in the  
809 CaSR cluster in three locations: (A) the TM1-TM2-TM7 interface, (B) the TM3 interface and (C) the  
810 TM6 interface. Those mutant residues that do not project towards the interface or are not interacting  
811 with other residues within the interface are not shown on the model.

812

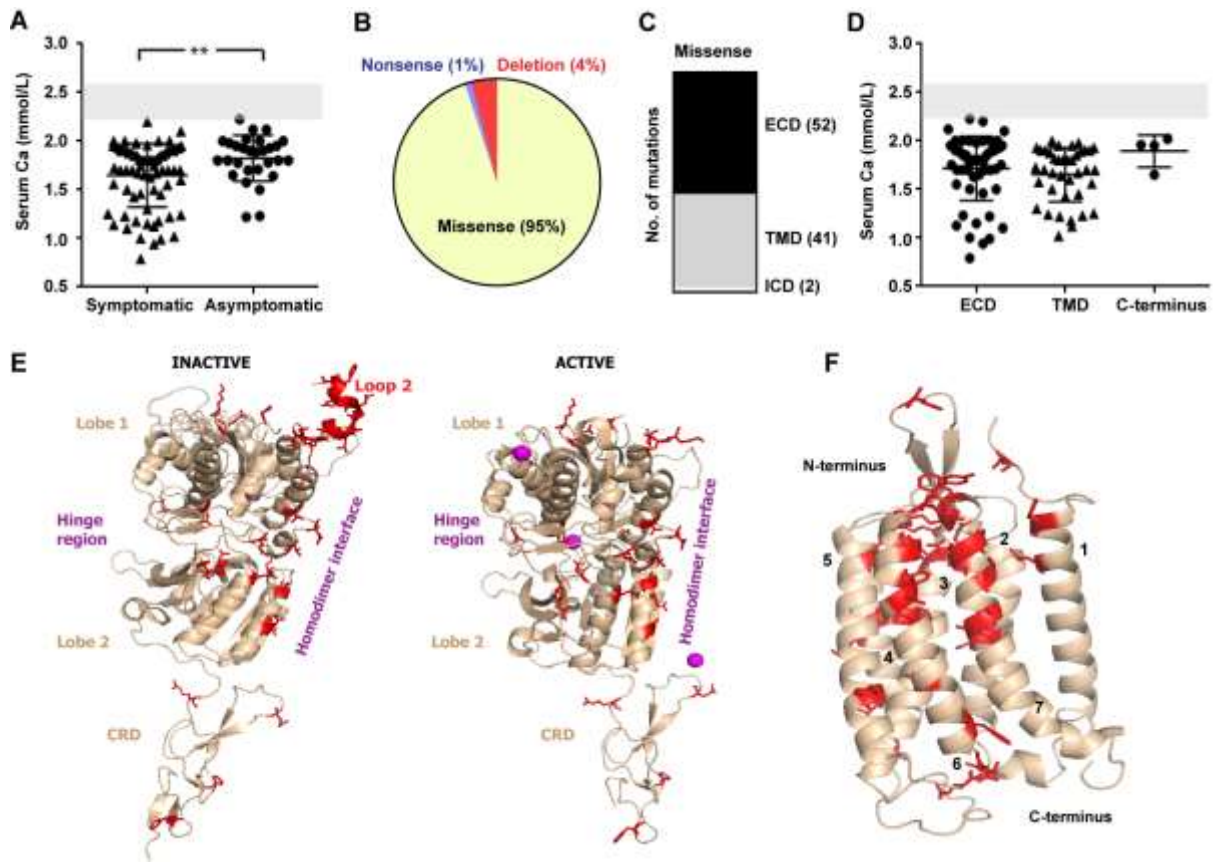


813

814 **FIGURE 6**

815 Genetic landscape of ADH1 mutations. (A) Mean serum calcium values of ADH1 patients with  
816 symptomatic vs. asymptomatic hypocalcaemia. Patients were regarded as symptomatic if they presented  
817 with signs of hypocalcaemia (e.g. carpopedal spasms, tetany, paraesthesia and seizures) or associated  
818 phenotypes (e.g. basal ganglia calcification). Patients with symptomatic hypocalcaemia have lower  
819 serum calcium values than asymptomatic individuals. Grey line indicates normal range values (2.2-2.6  
820 mmol/L). (B) Pie chart showing type of mutations described in ADH1 patients expressed as a  
821 percentage. The majority of mutations are missense, with a few cases of small deletions reported that  
822 affect the intracellular C-terminal region of the CaSR. (C) Location of the ADH1 missense mutations  
823 in the three CaSR domains. Similar numbers of ADH1 mutations affect the ECD and TMD of the  
824 receptor. (D) Serum calcium values of individuals with ADH1 mutations in each of the three domains  
825 of the CaSR showing no significant difference. (E) Model showing locations of the ADH-associated  
826 mutations (red sticks) in the inactive and active structures of the CaSR-ECD (PDB:5K5S) (Geng et al.  
827 2016). ADH1 mutations cluster in loop 2, the lobe 1-lobe 2 hinge region and the homodimer interface.  
828 Conformational changes occur primarily in the lobe 2 and CRD regions on ligand-binding, leading to  
829 an increase in residue contacts between the two protomers. (F) Homology model of the CaSR-TMD  
830 based on the crystal structure of mGluR5 (PDB:4OO9) (Dore et al. 2014) generated using Swiss-Model  
831 (<https://swissmodel.expasy.org/>). Residues mutated in ADH1 are shown in red, Ca<sup>2+</sup> bound to the  
832 structure is shown in magenta. The majority of ADH1 mutations are located in TM6, ECL2 and TM7,  
833 which undergo large structural changes on receptor activation in other GPCRs. Biochemical data and  
834 information on mutations was obtained from the references shown in Supplementary Table 1).  
835 Statistical analyses were performed by Student's t-test or one-way ANOVA. \*\*p<0.01.

836



837